ISSN 1070-3284, Russian Journal of Coordination Chemistry, 2023, Vol. 49, No. 9, pp. 528–541. © Pleiades Publishing, Ltd., 2023.
Russian Text © The Author(s), 2023, published in Koordinatsionnaya Khimiya, 2023, Vol. 49, No. 9, pp. 516–529.

Cytotoxic Copper(II) Complexes Based on 2,2'-Bipyridine/1,10-Phenanthroline and 5-(4-Chlorophenyl)-1*H*-tetrazole: Synthesis and Structures

Yu. A. Golubeva[a], K. S. Smirnova[a], L. S. Klyushova[b], A. S. Berezin[a], and E. V. Lider[a, *]

[a] *Nikolaev Institute of Inorganic Chemistry, Siberian Branch, Russian Academy of Sciences, Novosibirsk, Russia*

[b] *Research Institute of Molecular Biology and Biophysics, Federal Research Center of Fundamental and Translational Medicine, Novosibirsk, Russia*

**e-mail: lisalider@ngs.ru*

Received December 22, 2022; revised January 17, 2023; accepted January 17, 2023

Abstract—Five coordination compounds $[Cu_2(Bipy)_2L_4]\cdot C_2H_5OH$ (**Ia**, **Ib**), $[Cu_2(Dmbipy)_2L_4]$ (**II**), $[Cu_2(Phen)_2L_4]\cdot H_2O$ (**IIIa**), $[Cu_2(Dmphen)_2L_4]$ (**IVa**), and $[Cu_2(Phendione')_2L_4]\cdot 2C_2H_5OH\cdot 2H_2O$ (**V**) are synthesized from 5-(4-chlorophenyl)-1*H*-tetrazole (HL), where Bipy is 2,2'-bipyridine, Dmbipy is 4,4'-dimethyl-2,2'-bipyridine, Phen is 1,10-phenanthroline, Dmphen is 4,7-dimethyl-1,10-phenanthroline, and Phendione' is 6-ethoxy-6-hydroxy-1,10-phenanthrolin-5-one. The crystal structures of the complexes are determined by X-ray diffraction (XRD) of single crystals (CIF files CCDC nos. 2225368 (**Ia**), 2225369 (**Ib**), 2225370 (**II**), 2225372 (**IIIa**), 2225373 (**IVa**), and 2225371 (**V**)). The compounds are binuclear due to the bridging function of the tetrazolate anion, and the coordination number of copper is five in all synthesized complexes. The cytotoxic activity of the complexes against the Hep2 and HepG2 cancer cell lines and non-cancerous human fibroblasts MRC-5 is studied. The complexes exhibit pronounced cytotoxic properties, and compound **V** has the maximum selectivity index with respect to the cancer cells.

Keywords: copper(II) complexes, 5-(4-chlorophenyl)-1*H*-tetrazole, 1,10-phenanthroline, XRD, cytotoxicity

DOI: 10.1134/S1070328423600110

INTRODUCTION

The application of coordination compounds as promising pharmaceuticals for the diagnosis and treatment of cancer diseases is of current interest. The discovery of the inhibitory effect of *cis*-$[Pt(NH_3)_2Cl_2]$ (cisplatin) on the cancer cell growth in the 1960s [1] became an important milestone in the use of complexes in medicine. Cisplatin has widely been used up to now in the chemotherapy of some types of cancer along with the later developed carboplatin, oxaliplatin, nedaplatin, and other platinum-based drugs [2]. However, the range of malignant tumors, which can be treated by these compounds, is rather narrow, and serious side effects (neurotoxicity, ototoxicity, thrombocytopenia, and others) and resistance to therapy with similar drugs additionally restrict their application [3]. Unsolved problems related to chemotherapy by the platinum-based drugs result in a necessity of developing new compounds with an alternative mechanism of action for the improvement of the clinical efficiency, a decrease in the total toxicity, and extension of the activity spectrum.

Interest in coordination copper compounds increased multiply due to the capability of a series of the complexes of binding with DNA [4, 5], inhibiting topoisomerases [6], and generating reactive oxygen and nitrogen species [7, 8], which leads to the oxidative damage and death of cells. Therefore, many copper(II) complexes with diverse N,O,S-donor ligands, which have cytotoxic properties against cancer cell lines, were synthesized [8–16]. In addition, a significant body of studies is devoted to the coordination copper(II) compounds based on 2,2'-bipyridine (Bipy) and 1,10-phenanthroline (Phen) [17–24]. In particular, one of the copper(II) complexes belonging to a series of compounds named Casiopeinas with the general formula $[Cu(L^1)(L^2)]NO_3$ (L^1 is Bipy/Phen or their derivatives, L^2 is acetylacetonate or amino acid anion) exhibits a significant cytotoxic activity in vitro and in vivo and now is at the phase I clinical trials [18]. In addition, it is shown [25] that for this class of complexes the binding mode with DNA is determined by the type of ligand L^2 and also depends on the presence of electron-donating or electron-withdrawing substituents in ligand L^1. Thus, the variation of ligand L^2 in the copper(II) complexes with Bipy/Phen can favor the enhancement of the anticancer properties of the

compounds and can change their mechanism of action.

The purpose of this work is the synthesis and characterization of the cytotoxic copper(II) complexes with Bipy, 4,4'-dimethyl-2,2'-bipyridine (Dmbipy), Phen, 4,7-dimethyl-1,10-phenanthroline (Dmphen), and 6-ethoxy-6-hydroxy-1,10-phenanthrolin-5-one (Phendione'), where the second ligand is the tetrazole derivative: 5-(4-chlorophenyl)-1*H*-tetrazolate anion.

EXPERIMENTAL

Commercially available reagents were used for the synthesis of the complexes: 5-(4-chlorophenyl)tetrazole (HL), 1,10-phenanthroline monohydrate, and 2,2'-bipyridine (reagent grade); 4,4'-dimethyl-2,2'-bipyridine, 4,7-dimethyl-1,10-phenanthroline, 1,10-phenanthroline-5,6-dione, and 5-(4-chlorophenyl)-1*H*-tetrazole (high-purity grade) (their structural formulas are shown in Scheme 1); $Cu(OAc)_2 \cdot H_2O$ (analytical grade); and ethanol (rectificate).

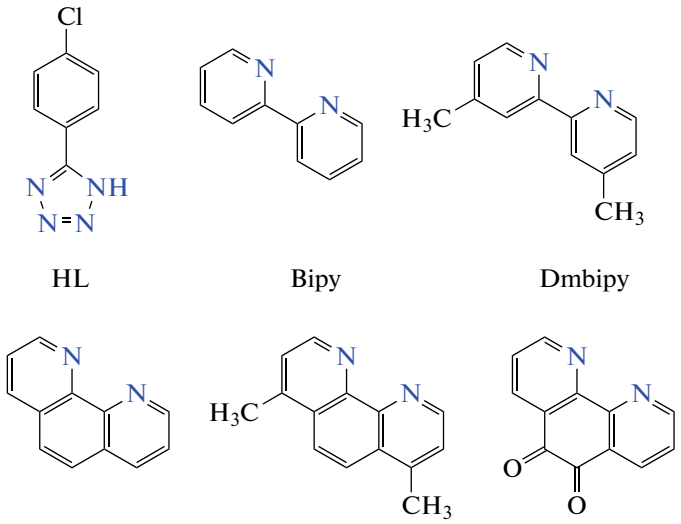

Scheme 1.

Heteroligand complexes $[Cu_2(Bipy)_2L_4]$ (CIF file CCDC no. 1551671) and $[Cu_2(Phen)_2L_4] \cdot (CH_3)_2NC(O)H$ (CIF file CCDC no. 1551672) were synthesized earlier [26] by the [2 + 3] cycloaddition between 4-chlorobenzonitrile the and azide ion coordinated to the copper atom in the $[Cu_2(Bipy/Phen)_2(N_3)_4]_n$ complex.

The synthesis was carried out by mixing aqueous-ethanol solutions of copper(II) acetate and the corresponding ligands shown in Scheme 1.

Synthesis of $[Cu_2(Bipy)_2L_4] \cdot C_2H_5OH$ (I). Weighed samples of copper(II) acetate (0.20 mmol, 0.040 g) and 2,2'-bipyridine (0.20 mmol, 0.031 g) were mixed and dissolved in an ethanol–water (1 : 1) mixture (4 mL) on heating to 60°C. The resulting dark blue solution was magnetically stirred for 5 min. An ethanolic solution (4 mL) of 5-(4-chlorophenyl)tetrazole (0.40 mmol, 0.072 g) was poured to the mixture. The formed blue precipitate of compound **I** was filtered off, washed with ethanol, and dried in air. Dark blue crystals of $[Cu_2(Bipy)_2L_4] \cdot 2C_2H_5OH$ (**Ia**) precipitated in a week from the mother liquor, and crystals of $[Cu_2(Bipy)_2L_4] \cdot 2(CH_3)_2SO$ (**Ib**) were obtained by recrystallization from a DMSO solution. The yield was 0.10 g (83%).

IR (ν, cm^{-1}): 3441 ν(OH); 3057, 2955, 2924 ν(CH); 1603, 1568, 1515, 1498 R_{rings}; 1090 ν(C–Cl). DRS: $\lambda_{max} = 600$ nm.

For $C_{50}H_{38}N_{20}OCl_4Cu_2$			
Anal. calcd., %	C, 49.9	H, 3.2	N, 23.3
Found, %	C, 49.3	H, 3.4	N, 23.1

Synthesis of $[Cu_2(Dmbipy)_2L_4]$ (II) was conducted according to a procedure similar to that for compound **I** using 4,4'-dimethyl-2,2'-bipyridine instead of 2,2'-bipyridine. Dark blue crystals of compound **II** were obtained from the mother liquor in a week. The yield of compound **II** was 0.090 g (74%).

IR (ν, cm^{-1}): 3126, 3071, 3028, 2924 ν(CH); 1618, 1562, 1516, 1496 R_{rings}; 1090 ν(C–Cl). DRS: $\lambda_{max} = 634$ nm.

For $C_{52}H_{40}N_{20}Cl_4Cu_2$			
Anal. calcd., %	C, 51.4	H, 3.3	N, 23.1
Found, %	C, 51.6	H, 3.3	N, 23.1

Synthesis of $[Cu_2(Phen)_2L_4] \cdot H_2O$ (III) was conducted according to a procedure similar to that for compound **I** using 1,10-phenanthroline instead of

2,2'-bipyridine. Dark blue crystals of $[Cu_2(Phen)_2L_4]\cdot 2C_2H_5OH$ (**IIIa**) were obtained from the mother liquor in a week. The yield of compound **III** was 0.15 g (82%).

IR (ν, cm^{-1}): 3319 ν(OH); 3086, 3060, 3017, 2962 ν(CH); 1627, 1607, 1585, 1519 R_{rings}; 1093 ν(C–Cl). DRS: λ_{max} = 622 nm.

For $C_{52}H_{34}N_{20}OCl_4Cu_2$			
Anal. calcd., %	C, 51.0	H, 2.8	N, 22.9
Found, %	C, 51.1	H, 2.9	N, 22.5

Synthesis of $[Cu_2(Dmphen)_2L_4]$ (IV) was conducted according to a procedure similar to that for compound **I** using 4,7-dimethyl-1,10-phenanthroline instead of 2,2'-bipyridine. Crystals of $[Cu_2(Dmphen)_2L_4]\cdot 2.5(CH_3)_2SO\cdot H_2O$ (**IVa**) were obtained from a DMSO solution upon recrystallization. The yield of compound **IV** was 0.10 g (79%).

IR (ν, cm^{-1}): 2953, 2924, 2854 ν(CH); 1622, 1614, 1541, 1505 R_{rings}; 1080 ν(C–Cl). DRS: λ_{max} = 639 nm.

For $C_{56}H_{40}N_{20}Cl_4Cu_2$			
Anal. calcd., %	C, 53.3	H, 3.2	N, 22.2
Found, %	C, 53.3	H, 3.0	N, 22.4

Synthesis of $[Cu_2(Phendione')_2L_4]\cdot 2C_2H_5OH\cdot 2H_2O$ (V) was conducted according to a procedure similar to that for compound **I** using 1,10-phenanthroline-5,6-dione instead of 2,2'-bipyridine. An ethanol molecule adds to Phendione during the synthesis due to which 6-ethoxy-6-hydroxy-1,10-phenanthrolin-5-one (Phendione') enters the complex. The complex was isolated from the reaction mixture in a week as blue-gray crystals. The yield of compound **V** was 51%.

IR (ν, cm^{-1}): 3350, 3280, 3160 ν(OH); 3098, 3065, 3030, 2970, 2922, 2893 ν(CH); 1715, 1670 ν(C=O); 1609, 1580, 1518, 1489 R_{rings}; 1032 ν(C–Cl). DRS: λ_{max} = 645 nm.

For $C_{60}H_{56}N_{20}O_{10}Cl_4Cu_2$			
Anal. calcd., %	C, 48.5	H, 3.8	N, 18.9
Found, %	C, 48.2	H, 3.5	N, 19.2

Elemental (C, H, N) analysis was carried out at the Analytical Laboratory of the Nikolaev Institute of Inorganic Chemistry (Siberian Branch, Russian Academy of Sciences) on a Vario MICRO cube analyzer. The IR spectra of the samples prepared as suspensions in Nujol and fluorinated oil were recorded on a Scimitar FTS 2000 FT-IR spectrometer in a range of 4000–400 cm^{-1}.

Powder XRD was carried out on a Shimadzu XRD-7000S diffractometer (CuK_α radiation, λ = 1.54056 Å, Ni filter, measurement 2θ range from 5° to 40°, acquisition 1 s per point).

The electronic absorption spectra of a solution of compound **II** were recorded on an SF-102 spectrometer in a range of 200–900 nm at room temperature (solvent DMSO, c = 1 mM). For recording spectra in the UV range, a concentrated solution of the complex in DMSO was diluted with water to a concentration of 15 μM.

Diffuse reflectance spectra (DRS) were recorded on a Shimadzu UV-3101 instrument at room temperature in a range of 250–1200 nm. The initial dependences of the reflection of the samples (R) on the wavelength were recalculated using the Kubelka–Munk function (M) by the equation $M = \frac{(1-R)^2}{2R}$.

EPR spectra were recorded in the Q frequency range at 300 K on a Varian E-109 automated spectrometer. 1,1-Diphenyl-2-picrylhydrazyl served as the standard. EPR spectra were processed using the software for Matlab–EasySpin [27]. EPR spectra were recorded for polycrystalline samples and for a frozen solution of complex **I** (solvents DMSO, ethanol (1 : 10), X range, T = 77 K).

XRD for single crystals of compounds **Ib**, **II**, **IIIa**, **IVa**, and **V** was carried out on a Bruker D8 Venture diffractometer (MoK_α radiation, λ = 0.71073 Å) at T = 150 K. Reflection intensities were measured in the φ and ω scan modes. The data were integrated and an absorption correction was applied using the SADABS software [28]. The XRD data for compound **Ia** were obtained on an Agilent Xcalibur diffractometer equipped with an AtlasS2 detector (monochromatic graphite MoK_α radiation, λ = 0.71073 Å) at T = 150 K. Integration was performed, an absorption correction was applied, and unit cell parameters were determined using the CrysAlisPro program [29]. The structures were solved and refined using the SHELXT [30] and SHELXL [31] programs in the OLEX2 graphical interface [32]. Non-hydrogen atoms were refined in the anisotropic approximation. Hydrogen atoms were localized geometrically and refined by the riding model. Complex **IVa** contains disordered DMSO and water molecules. As a result, the hydrogen atoms were not localized for the water molecules but were included into the empirical formula of the compound. In complex **V**, the ethoxy group is disordered over two positions with a population ratio of 2 : 3. The system also exhibits the disordering of the phenyl group of one of molecules L^- over two positions with the population ratio 3 : 7. Some restraints were additionally applied: on the bond length (SADI), on the planar fragment of the phenyl group (FLAT), on the anisotropy of selected atoms (ISOR, EADP), and on the rigidity of the bond between the atoms (RIGU). In compound **V**, the ethanol molecule is disordered over at least four positions. As a result, the Solvent Mask function was applied in the OLEX2 program for the removal of the electron density corresponding to two ethanol molecules in the system. The crystallographic data and information on the refined structures are given in Table 1.

The full set of XRD parameters was deposited with the Cambridge Crystallographic Data Centre (CIF files CCDC nos. 2225368 (**Ia**), 2225369 (**Ib**), 2225370 (**II**), 2225372 (**IIIa**), 2225373 (**IVa**), and 2225371 (**V**); http://www.ccdc.cam.ac.uk/data_request/cif).

Study of cytotoxic activity. The Hep2 (human laryngeal carcinoma cells), HepG2 (human hepatocarcinoma cells), and MRC-5 (human fibroblast cell line) cell lines were cultivated in a CO_2 incubator (5% CO_2 and 95% air) at 37°C in 96-well plates in an IMDM medium containing a 10% additive of fetal bovine serum. The complexes and ligands were dissolved in DMSO, and working solutions were prepared by the serial dilution method with an IMDM nutrient medium. After 24 h of cultivation, the preparations were added to the cells in a concentration range of 0.1–50 μM, and the resulting samples were incubated for 48 h. For the identification of living, apoptotic, and dead cells, the treated cells and control cells were dyed with a mixture of the fluorescent dyes Hoechst 33342 (Sigma-Aldrich) and propidium iodide (Invitrogen) at 37°C for 30 min. Detection was carried out on an IN Cell Analyzer 2200 instrument (GE Healthcare, UK) in the automated mode at least 4 fields per well with a 200-fold magnification in the brightfield channel and fluorescence channel. The obtained images were examined using the In Cell Investigator program. The result of the studies is presented as the percentage of the content of living, dead, and apoptotic cells from three independent experiments ± standard deviation.

RESULTS AND DISCUSSION

Complexes **I**–**V** were synthesized by the reactions of aqueous-ethanol solutions of copper(II) acetate and Bipy/Phen derivatives and 5-(4-chlorophenyl)tetrazole (HL) at the molar ratio of the reagents 1 : 1 : 2, respectively (Scheme 2). 1,10-Phenanthroline-5,6-dione was used for the synthesis of complex **V**, but the ethanol molecule adds to the C(6) atom of this ligand during the synthesis due to which 6-ethoxy-6-hydroxy-1,10-phenanthrolin-5-one (Phendione') enters the complex.

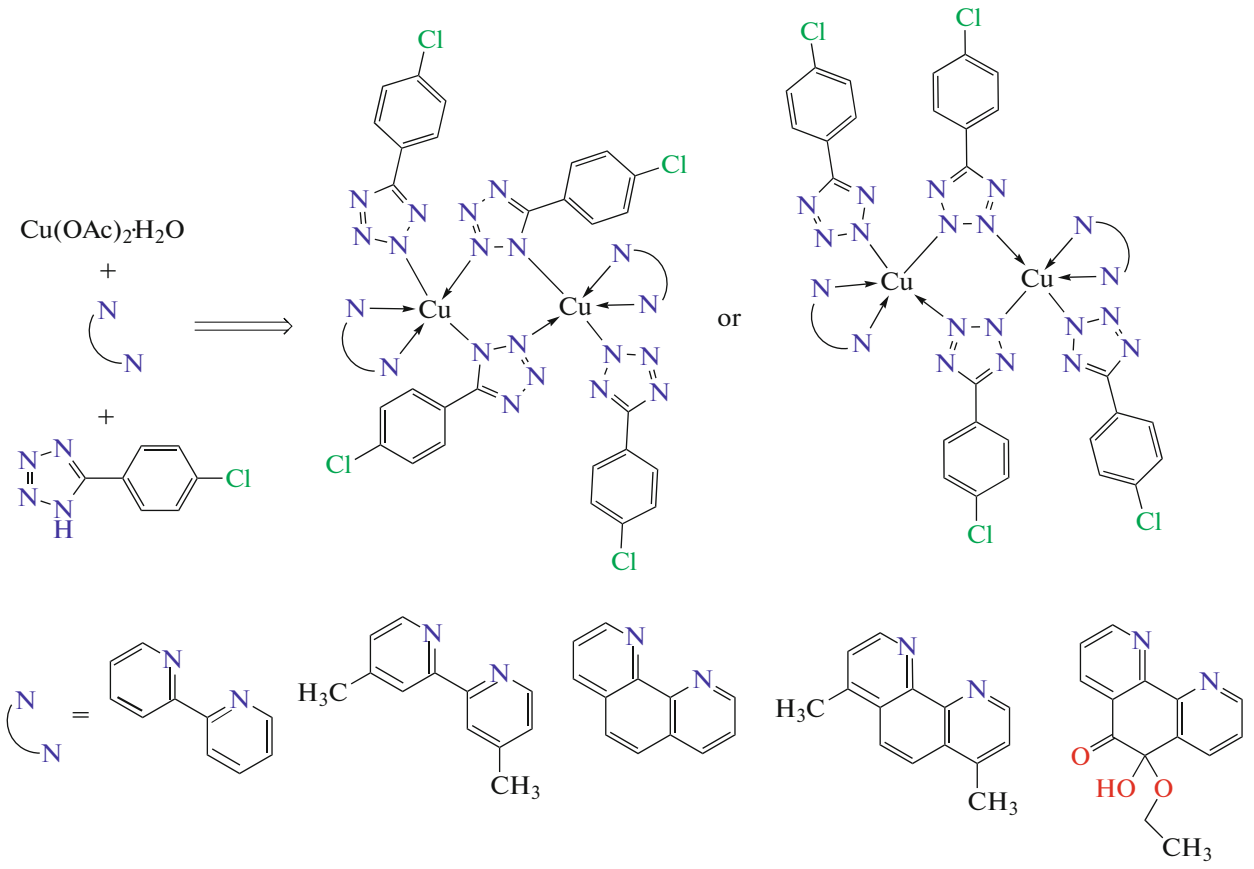

Scheme 2.

Complexes **I**–**V** are soluble in DMSO, poorly soluble in ethanol, and insoluble in water and a phosphate-buffer saline. Single crystals of $[Cu_2(Bipy)_2L_4]\cdot 2C_2H_5OH$ (**Ia**), $[Cu_2(Dmbipy)_2L_4]$ (**II**), $[Cu_2(Phen)_2L_4]\cdot C_2H_5OH$ (**IIIa**), and $[Cu_2(Phendione)_2L_4]\cdot 2C_2H_5OH\cdot 2H_2O$ (**V**) were obtained by the slow crystallization from aqueous-ethanol mother liquors, and those of $[Cu_2(Bipy)_2L_4]\cdot 2(CH_3)_2SO$ (**Ib**) and $[Cu_2(Dmphen)_2L_4]\cdot 2.5(CH_3)_2SO\cdot H_2O$ (**IVa**) were obtained by the recrystallization from a DMSO solution.

Table 1. Crystallographic data and experimental and structure refinement parameters for compounds **Ia**, **Ib**, **II**, **IIIa**, **IVa**, and **V**

Parameter	Value					
	Ia	**Ib**	**II**	**IIIa**	**IVa**	**V**
Empirical formula	$C_{52}H_{44}N_{20}O_2Cl_4Cu_2$	$C_{52}H_{44}N_{20}O_2S_2Cl_4Cu_2$	$C_{52}H_{40}N_{20}Cl_4Cu_2$	$C_{56}H_{44}N_{20}O_2Cl_4Cu_2$	$C_{61}H_{58}N_{20}O_4S_{2.5}Cl_4Cu_2$	$C_{56}H_{44}N_{20}O_8Cl_4Cu_2$
FW	1249.95	1314.07	1213.92	1297.99	1484.30	1393.99
Temperature, K	140	150	150	150	150	150
Crystal system	Monoclinic	Monoclinic	Monoclinic	Monoclinic	Triclinic	Triclinic
Space group	$P2_1/n$	$P2_1/c$	$P2_1/c$	$P2_1/c$	$P\bar{1}$	$P\bar{1}$
a, Å	13.8545(4)	15.9535(5)	16.639(2)	14.3370(7)	11.4815(6)	11.1984(3)
b, Å	9.8679(3)	16.5631(5)	10.2119(15)	16.9476(8)	15.8534(8)	12.2635(3)
c, Å	19.4659(4)	10.8352(3)	16.989(2)	11.4664(5)	19.0014(10)	13.1268(4)
α, deg	90	90	90	90	75.776(2)	98.9740(10)
β, deg	90.681(2)	103.3470(10)	113.173(4)	95.565(2)	88.857(2)	91.8370(10)
γ, deg	90	90	90	90	82.080(2)	115.5660(10)
V, Å^3	2661.09(12)	2785.75(14)	2653.9(6)	2772.9(2)	3320.3(3)	1596.29(8)
Z	2	2	2	2	2	1
ρ_{calc}, g/cm^3	1.560	1.567	1.519	1.555	1.480	1.450
μ, mm^{-1}	1.064	1.093	1.06	1.02	0.94	0.90
Crystal size, mm^3	0.3 × 0.14 × 0.12	0.11 × 0.06 × 0.01	0.13 × 0.03 × 0.01	0.20 × 0.04 × 0.01	0.10 × 0.06 × 0.01	0.11 × 0.09 × 0.04
Scan range over 2θ, deg	4.19–56.88	3.60–56.60	4.77–54.38	3.73–51. 8	3.02–49.56	4.06–63.16
Range of indices *hkl*	$-18 \le h \le 18$, $-12 \le k \le 11$, $-24 \le l \le 26$	$-21 \le h \le 21$, $-22 \le k \le 22$, $-14 \le l \le 12$	$-21 \le h \le 21$, $-12 \le k \le 13$, $-21 \le l \le 21$	$-17 \le h \le 17$, $-20 \le k \le 20$, $-13 \le l \le 13$	$-13 \le h \le 13$, $-18 \le k \le 18$, $-22 \le l \le 22$	$-16 \le h \le 16$ $-18 \le k \le 18$ $-19 \le l \le 19$
Number of reflections measured/independent	11 809/5800	3107/6928	26 136/5868	26947/5262	43 558/11 389	77952/10671
R_{int}	0.0197	0.0674	0.104	0.119	0.0950	0.0338
Number of restrains/ parameters	0/363	0/372	0/369	0/383	0/866	155/499
Goodness-of-fit for F^2	1.037	1.031	1.031	1.023	1.033	1.059
R_1, wR_2 ($I > 2\sigma(I)$)	0.0295, 0.0691	0.0426, 0.0862	0.0544, 0.1156	0.0543, 0.0964	0.0679, 0.1700	0.0460, 0.1293
R factors (all reflections)	0.0380, 0.0720	0.0689, 0.0973	0.1019, 0.1383	0.1036, 0.1147	0.1294, 0.2012	0.0531, 0.1354
Residual electron density (max/min), e Å^{-3}	0.33/–0.42	0.55/–0.47	0.44/–0.62	0.71/–0.55	0.90/–0.70	1.87/–1.18

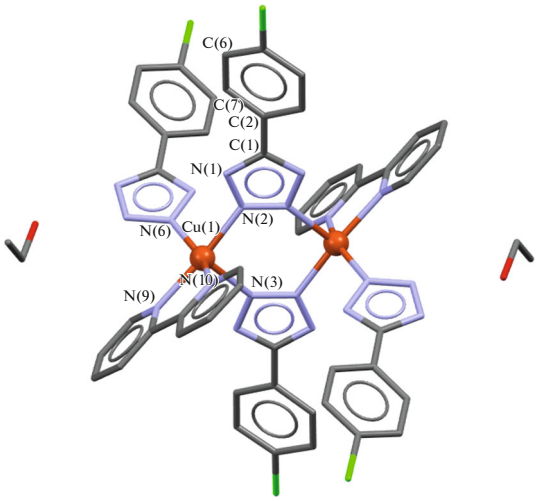

Fig. 1. Molecular structure of complex **Ia**. Hydrogen atoms are omitted.

Complexes **Ia** and **Ib** crystallize in the monoclinic system with the space groups $P2_1/n$ and $P2_1/c$, respectively. The independent part of the structures contains one copper atom, Bipy molecule and two L^- anions (Fig. 1). The copper atom exists in a square pyramidal environment of five nitrogen atoms, and the parameters of the SHAPE analysis $S(C_{4v})$ and τ_5 were 0.70 and 0.21 (**Ia**) and 0.48 and 0.065 (**Ib**). The Cu–N bond lengths in the basal plane vary from 1.9840(14) to 2.0464(15) Å for **Ia** and from 1.976(2) to 2.044(2) Å for **Ib** (Table 2). The coordination polyhedron exhibits a tetragonal distortion characteristic of the copper(II) complexes. For instance, the length of the Cu–N apical bond is 2.1868(15) Å in complex **Ia** and 2.214(2) Å in complex **Ib**. Two copper atoms are connected to each other via bridging ions L^- coordinated by the N(2) and N(3) atoms. The terminal tetrazolate ions coordinate to the copper(II) ion by the N(2) nitrogen atom. The distance between the copper(II) ions is 4.031 Å for complex **Ia** and 4.117 Å in complex **Ib**. The structures also contain solvate molecules of ethanol (**Ia**) and DMSO (**Ib**) (Fig. S1). The uncoordinated ethanol molecule in complex **Ia** forms a hydrogen bond with the nitrogen atom of the tetrazolate anion coordinated via the monodentate mode (2.962 Å).

The complex with a similar structure $[Cu_2(Bipy)_2L_4]$ (CIF file CCDC no. 1551671), which crystallizes in the triclinic system with the space group $P\bar{1}$ and contains no solvate molecules, can be found in the Cambridge Structural Database (CSD). The coordination of the bridging and terminal tetrazolate ion is the same in all three complexes. However, the superposition of these structures shows distinctions in the steric arrangement of the ligands (Fig. 2). In particular, significant differences in torsion angles are observed for the bridging ligand molecules. For instance, in the structures of complexes **Ia** and **Ib**, the N(1)–C(1)–C(2)–C(7) torsion angle is 22° and 27°, respectively; and this angle is 10° in the $[Cu_2(Bipy)_2L_4]$ structure from the CSD. In addition, the turn of the terminal ligand along the Cu–N(6) axis is observed in the case of complex **Ia**.

Complex **II** crystallizes in the monoclinic system with the space group $P2_1/c$. The independent part of the structure is similar to that for complex **Ib** (Fig. 3). However, the polyhedron of the central atom can be assigned to both a square pyramid ($S(C_{4v}) = 2.00$) and a trigonal bipyramid ($S(D_{3h}) = 2.03$; $\tau_5 = 0.46$). The environment of the copper atom consists of five nitrogen atoms, the Cu–N bond lengths vary from 1.995(3) to 2.061(3) Å (Table 2), but the Cu–N(1) bond length is 2.169(3) Å thus confirming the square pyramidal environment of the central atom. Unlike compounds **I(a,b)**, the bridging L^- ions in complex **II** connect the adjacent copper atoms by the N(1) and N(2) nitrogen atoms. As a result, the intramolecular π stacking (3.784 Å) is formed between the benzene ring of ligand L^- and pyridine fragment of the Dmbipy molecule (Fig. 3). The Cu–Cu distance in this complex is 4.029 Å.

As compound **II**, complex **IIIa** crystallizes in the monoclinic system with the space group $P2_1/c$. The independent part of the structure is similar to those for complexes **Ia**, **Ib**, and **II** (Fig. 4). The coordination sphere of the central atom consists of five nitrogen atom that form a square pyramid around the copper(II) atom ($S(C_{4v}) = 0.27$; $\tau_5 = 0.11$). The Cu–N bond lengths in the basal plane vary from 1.970(4) to 2.052(3) Å (Table 2), and the Cu–N apical bond length is 2.159(3) Å. As in the case of complexes **Ia** and **Ib**, the bridging 5-(4-chlorophenyl)tetrazolate ion is coordinated by the N(2) and N(3) atoms, and the distance between the copper(II) ions is 4.009 Å. The solvate ethanol molecule forms a hydrogen bond with the nitrogen atom of the tetrazolate anion coordinated via the monodentate mode (2.859 Å). The complex with a similar structure $[Cu_2(Phen)_2L_4]\cdot(CH_3)_2NC(O)H$ (CIF file CCDC no. 1551672), which crystallizes in the triclinic system with the space group $P\bar{1}$ and contains the uncoordinated DMSO molecule, was published in the CSD.

Complex **IVa** contains solvate DMSO and water molecules. Unlike the compounds presented above, complex **IVa** crystallizes in the triclinic system with the space group $P\bar{1}$. The unit cell contains two crystallographically nonequivalent molecules of compound **IVa**. The 5-(4-chlorophenyl)tetrazolate ion demonstrates the same coordination modes as in complexes **IIIa**, **Ia**, and **Ib**: the monodentate mode by the N(2) nitrogen atom of the tetrazole cycle and bidentate bridging mode where the N(2) and N(3) atoms are involved in coordination (Fig. 5). The distance between the copper(II) atoms in the first compound is 3.950 Å, and that in the second compound is 4.093 Å

Table 2. Distances Cu···Cu and Cu–N bond lengths (Å) in the complexes

Complex	Cu–N_{bas}*		Cu–N_{apic}*		Cu···Cu	
Ia	2.0057(14) 2.0464(15) 2.0022(15) 1.9840(14)		2.1868(15)		4.031	
Ib	2.028(2) 2.044(2) 1.996(2) 1.976(2)		2.214(2)		4.117	
II	2.043(3) 2.061(3) 1.995(3) 1.958(3)		2.169(3)		4.029	
IIIa	2.026(3) 2.052(3) 2.003(3) 1.970(4)		2.159(3)		4.009	
IVa	Cu(1)–N 2.009(5) 2.035(4) 1.998(5) 1.979(5)	Cu(2)–N 2.013(5) 2.032(5) 2.000(5) 1.990(5)	Cu(1)–N 2.217(5)	Cu(2)–N 2.203(5)	Cu(1)...Cu(1) 3.950	Cu(2)...Cu(2) 4.093
V	2.0187(15) 2.0290(15) 2.0011(15) 1.9795(15)		2.2725(15)		4.110	

* bas is basal atom, and apic is apical atom.

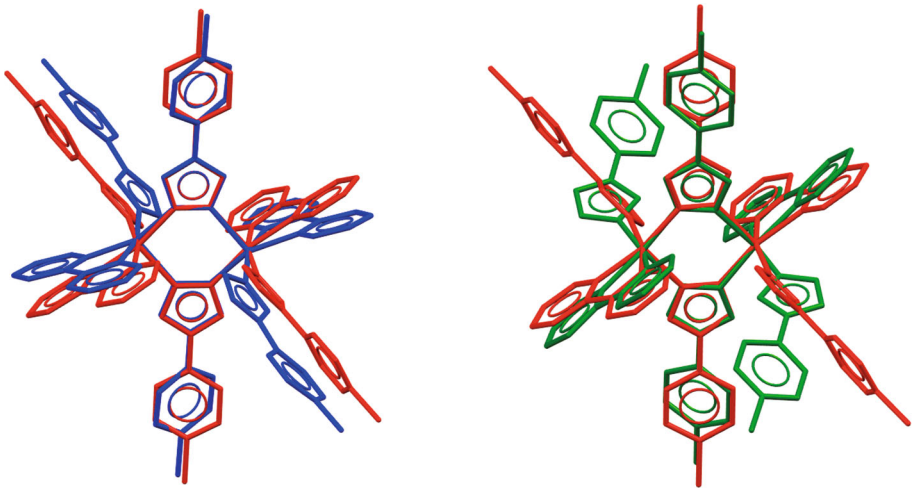

Fig. 2. Superposition of the crystal structures of complexes $[Cu_2(Bipy)_2L_4]$ (CSD, red), **Ib** (blue), and **Ia** (green). Solvent molecules are omitted.

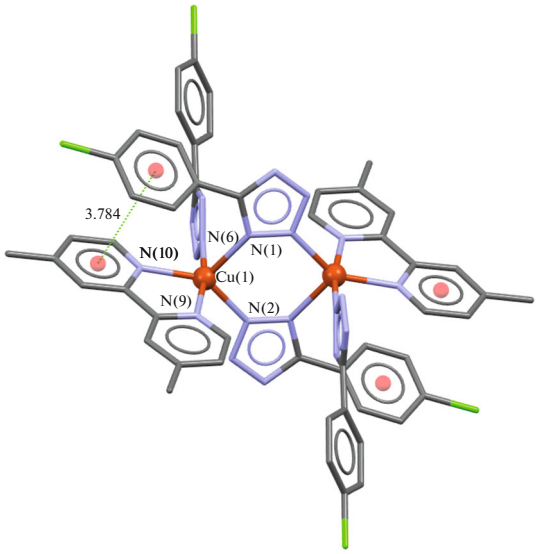

Fig. 3. Molecular structure of complex **II**. Hydrogen atoms are omitted.

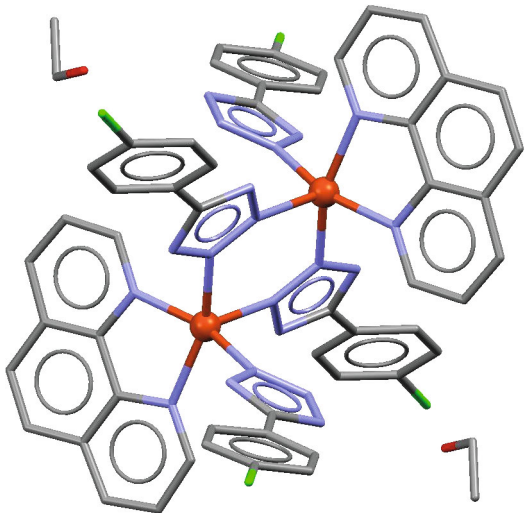

Fig. 4. Molecular structure of complex **IIIa**. Hydrogen atoms are omitted.

(Table 2). The coordination polyhedron of the central atom is a square pyramid with the parameter $S(C_{4v}) = 0.79$ for Cu(1) and 0.38 for Cu(2). In the basal plane, the Cu–N bond lengths vary from 1.979(5) to 2.035(4) Å and the Cu–N apical bond length is 2.217(5) Å for Cu(1) and 2.203(5) Å for Cu(2).

According to the XRD data, binuclear copper(II) complex **V** resembles the previous compounds. In the structure of complex **V**, the distance between the metal ions is 4.110 Å (Fig. 6) and the 5-(4-chlorophenyl)tetrazolate ion acts as the bridging (coordination by the N(2) and N(3) atoms) and terminal ligand (the N(2) nitrogen atom is involved in the coordination). Significant changes occurred with the 1,10-phenanthroline-5,6-dione molecule during the synthesis: a bond between the carbon atom of one of the carbonyl group and the ethanol molecule was formed, and the carbon atom became sp^3-hybrid. The structure contains uncoordinated water molecules forming hydrogen bonds with the nitrogen atoms of the tetrazole cycles of the bridging (O···N = 2.852 Å) and terminal (O···N = 2.917 Å) ligands. The coordination environment of copper(II) consisting of five nitrogen atoms can be considered as a square pyramid ($S(C_{4v}) = 0.74$; $\tau_5 = 0.04$), as well as the vacant octahedron ($S(C_{4v}) = 0.83$). Since the distance between the central atom and oxygen atom of the water molecule is 2.861 Å, the polyhedron of the copper(II) ion can be described as a distorted octahedron with the 5 + 1 environment ($S(O_h) = 2.03$).

According to the XRD data, complexes **I**–**V** are crystalline. The XRD patterns of complexes **II** and **V** are consistent with those calculated from the XRD data (Fig. S2). Selected reflections in the XRD pattern of complex **III** are shifted relative to the reflections in the XRD pattern calculated for $[Cu_2(Phen)_2L_4]\cdot(CH_3)_2NC(O)H$ (CIF file CCDC no. 1551672), which is probably a consequence of the influence of the solvate molecules on the packing of the complex molecules in the crystal (Fig. S3). The experimental XRD pattern of complex **IV** does not correspond to that calculated for single crystals of compound **IVa** obtained by the recrystallization of complex **IV** from DMSO (Fig. S4). The experimental XRD pattern of complex **I** does not either coincide with the calculated XRD patterns for **Ia**, **Ib**, and complex $[Cu_2(Bipy)_2L_4]$ found in the CSD (CIF file

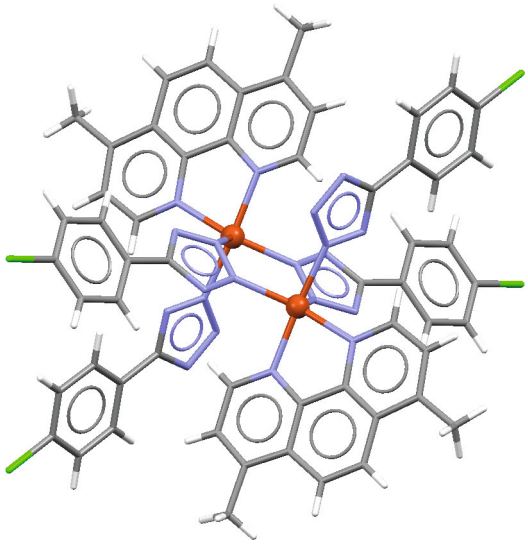

Fig. 5. Molecular structure of complex **IVa**. Uncoordinated DMSO and water molecules are omitted.

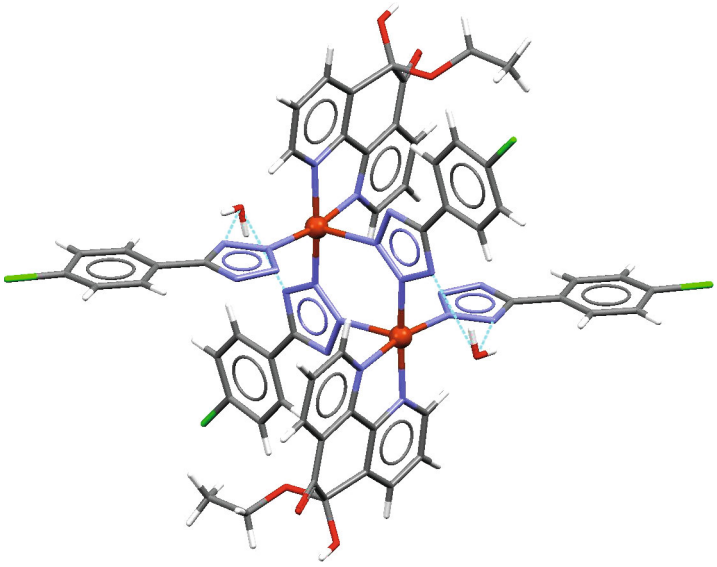

Fig. 6. Molecular structure of complex **V**. Ethanol molecules are omitted.

CCDC no. 1551671) (Fig. 7). This can be related to both the influence of the solvate molecules and existence of different conformers of this binuclear molecule, which is illustrated in Fig. 2.

The EPR spectra for polycrystalline complexes **I**–**V** (Fig. 8) were recorded at room temperature in the Q frequency range. The EPR spectra of complexes **I**–**IV** are described by the spin-Hamiltonian $\hat{H} = \beta Bg\hat{S} + D\left[\hat{S}_z^2 - \frac{S(S+1)}{3}\right] + E\left[\hat{S}_x^2 - \hat{S}_y^2\right]$ with the parameters given in Table 3. The EPR spectra with $S = 1$ and $|D| \neq 0$ indicate the dipole–dipole interaction between the copper(II) ions. In the framework of the point dipole model using the equation $D = \frac{2g_z^2 + \left(g_x^2 + g_y^2\right)/2}{2r_{\text{Cu-Cu}}^3}\beta^2$, the distances between the copper(II) ions can be estimated as ≈5.9 and 5.6 Å for complexes **I** and **II** based on 2,2'-bipyridine and ≈5.0 and 4.9 Å for complexes **III** and **IV** based on 1,10-phenanthroline (Table 3). The obtained values of r(Cu–Cu) somewhat exceed the distances between the copper(II) ions determined from the XRD data (r(Cu–Cu) ≈ 4.0 Å). In spite of this, the EPR spectroscopy data together with the XRD data indicate the binuclear structures of complexes **I**–**IV**.

The EPR spectrum of complex **V** is described by the spin-Hamiltonian $\hat{H} = \beta Bg\hat{S}$ with the parameters $S = 1/2$, $g_\perp = 2.064$, and $g_\parallel = 2.255$. The obtained spectrum resolved by the g tensor having no splitting in the zero field is characteristic of the mononuclear copper(II) complexes. In spite of the absence of a dipole-dipole interaction between the paramagnetic centers, according to the XRD data, complex **V** is binuclear with a short distance between the copper atoms (r(Cu–Cu) = 4.11 Å). A similar discrepancy between the data of XRD and EPR spectroscopy was observed earlier for analogous binuclear copper(II) complexes with the 5-phenyltetrazolate anion [33, 34].

To study the behavior of the complexes in a solution, we recorded the EPR spectrum for a frozen solution of complex **I** (solvents: DMSO, ethanol (1 : 10), X range, T = 77 K). The EPR spectrum (Fig. 9) is described by the spin-Hamiltonian $\hat{H} = \beta Bg\hat{S} + \sum \hat{I}A_i\hat{S}$ with the parameters $S = 1/2$, $g_x = g_y = 2.059$, $g_z = 2.275$, A_z(Cu) = 500 MHz, A_x(N) = A_y(N) = 41 MHz, and n(N) = 4. The spectrum exhibits a hyperfine structure from one copper ion and four equivalent nitrogen atoms. Thus, ligand redistribution can occur in the solution to form a species of the complex containing four equivalent nitrogen atoms, for example, $[Cu(Bipy)_2]^{2+}$ or $[CuL_4]^{2-}$.

The DRS and electronic absorption spectra in a DMSO solution in the visible spectral range were recorded for complexes **I**–**V**. The band maxima of d–d transitions for complexes **I**–**V** lie in a range of 600–645 nm, and the band of d–d transitions undergoes a low-frequency shift (λ_{max} = 678 nm) in a DMSO solution. A cause for similar shift of the absorption band maxima in a solution can be the coordination to the copper(II) ions of the ligands of a weaker field compared to oligopyridines and tetrazoles (solvent molecules).

The stability of the species of the complex existing in a solution was studied for complex **II**. For this purpose, the absorption spectra were recorded at the initial moment and in 24 and 48 h in the visible (DMSO solution) and UV (aqueous solution prepared by the

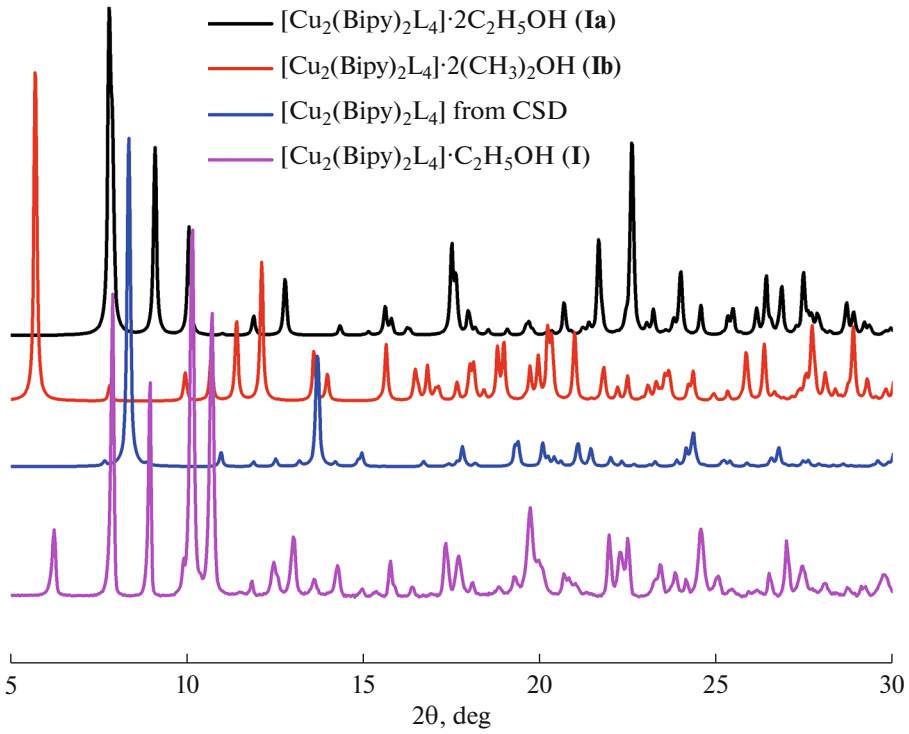

Fig. 7. XRD patterns calculated from the XRD data of single crystals of compounds **Ia** (black line), **Ib** (red line), and $[Cu_2(Bipy)_2L_4]$ (CCDC 1551671, blue line) and experimental (pink line) powder XRD pattern of complex **I**.

dilution of a DMSO solution (DMSO : water = 1 : 65 vol/vol)) ranges (Fig. 10). No changes in the absorption intensity or no shifts of the absorption band maxima are observed in the spectra within this time interval indicating that solutions of the complexes are stable for 48 h in both an aqueous solution and DMSO.

The cytotoxic activity of the complexes was estimated by high-content screening on an IN Cell Analyzer 2200 (double dyeing with the fluorescent dyes Hoechst and propidium iodide). The data obtained are given in Table 4 as the parameter IC_{50}: the concentration of the compound decreasing the number of living cells by 50% compared to the control.

Complexes **I**–**V** were shown to possess a pronounced dose-dependent cytotoxicity against the human laryngeal carcinoma (Hep2) and hepatocarcinoma (HepG2) cells, which is comparable and exceeds, in some cases, the activity of the cisplatin drug used as a reference compound. The effect of the complexes depends on what Bipy/Phen derivative enters the compound and enhances in the series Bipy < Dmbipy < Phen < Dmphen < Phendione. Copper(II) acetate and the tetrazole derivative are not toxic in a concentration range of 1–50 μM. The Bipy/Phen derivatives were found [35] to be capable of inducing cancer cell death. However, a comparison of

Table 3. Parameters of the EPR spectra for complexes **I**–**V**

Complex	S	g_x	g_y	g_z	$\|D\|$, MHz	$\|E\|$, MHz	r(Cu–Cu), Å
I	1	2.049	2.067	2.25	448	134	5.9
II	1	2.022	2.105	2.245	560	19	5.6
III	1	2.032	2.088	2.27	728	170	5.0
IV	1	2.031	2.084	2.25	784	235	4.9
V	1/2	2.064	2.064	2.255			

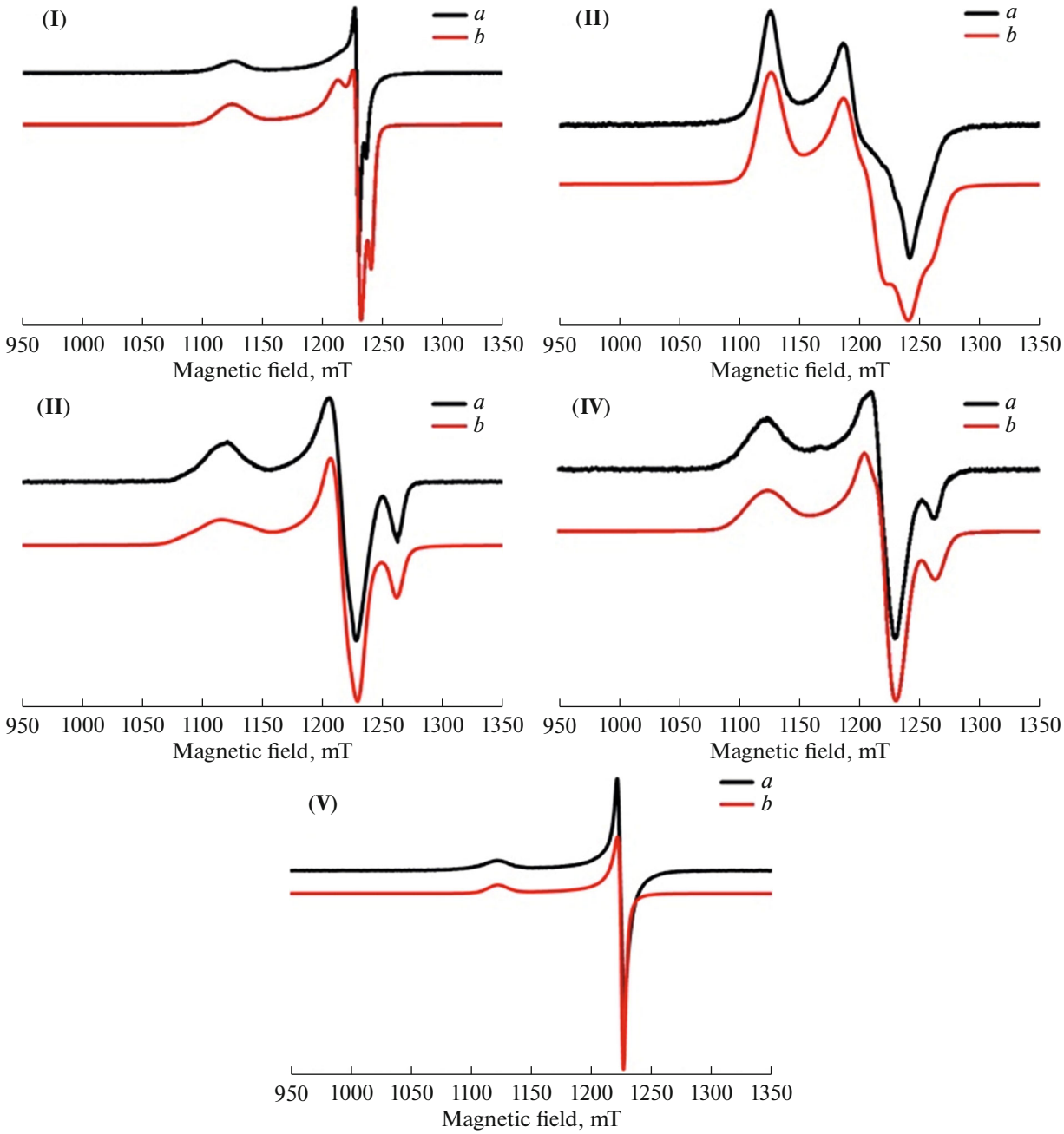

Fig. 8. EPR spectra in the Q frequency range for polycrystalline samples **I**–**V** at 300 K: (a) experimental and (b) simulated.

the parameters IC_{50} for these ligands and complexes shows an enhancement of the cytotoxic properties upon complex formation.

The cytotoxicity of compounds **I**–**V** was studied additionally on the noncancerous human fibroblasts MRC-5, and the selectivity indices were calculated as the ratio of the parameter IC_{50}(MRC-5) to IC_{50}(Hep2/HepG2). A selectivity was observed only for compound **V** (selectivity index >3).

The cytotoxic activity of structurally related binuclear complexes based on 5-phenyltetrazole $[Cu_2(L^1)_2(5\text{-phenyltetrazolate})_4]$ was studied [35]. The diagram with the values of IC_{50} on the HepG2 cells for the copper(II) complexes with different Bipy/Phen derivatives and 5-phenyltetrazole/5-(4-chlorophenyl)tetrazole is shown in Fig. 11. The activities of the compounds on this cell line are close. However, compounds **I** and **II** based on Bipy and Dmbipy exert a more pronounced effect on the cells compared

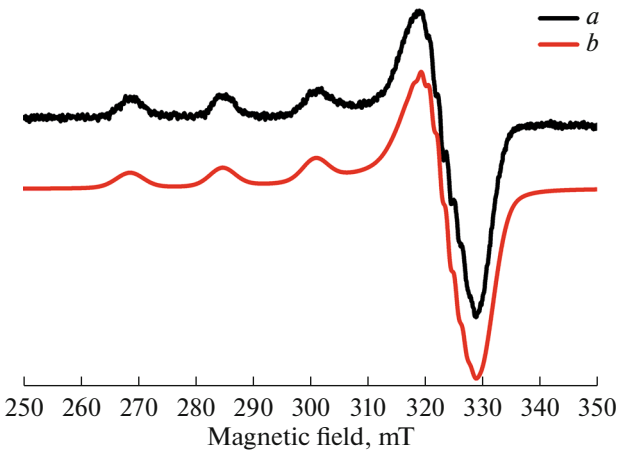

Fig. 9. EPR spectrum of a frozen solution of complex **I** (ethanol–DMSO (1 : 10) mixture) at 77 K in the X range: (a) experimental and (b) simulated.

to similar complexes based on 5-phenyltetrazole. An inverse pattern is observed for the compounds based on Phen and Phendione.

Thus, five binuclear copper(II) complexes based on the Bipy/Phen derivatives and tetrazole were synthesized and structurally characterized. The compounds were characterized by EPR and IR spectroscopy, elemental analysis, and XRD. The XRD method shows that two copper atoms are linked by the bridging 5-(4-chlorophenyl)tetrazolate anions coordinated via the N(2), N(3) or N(1), N(2) atoms (in the case of complex **II** with Dmbipy). The tetrazolate ions coordinate to the terminal copper(II) ions by the N(2) nitrogen atom, as well as the 2,2'-bipyridine/1,10-phenanthroline derivatives. The stability of aqueous solutions of the complexes within 48 h was demonstrated by optical spectroscopy. The synthesized compounds were found to possess pronounced cytotoxic properties against the cancer cell lines.

ACKNOWLEDGMENTS

The authors are grateful to A.P. Zubareva and N.N. Komardina for elemental analysis data; to A.S. Sukhikh, T.S. Sukhikh, V.Yu. Komarov, and V.N. Yudin for kindly presented data measured at the X-ray Diffraction Center for Collective Use of the Nikolaev Institute of Inorganic Chemistry (Siberian Branch, Russian Academy of Sciences); to D.G. Samsonenko for the XRD data for complex **Ia**; and to M.O. Matveeva for performing powder XRD.

FUNDING

This work was supported by the Ministry of Science and Higher Education of the Russian Federation (project

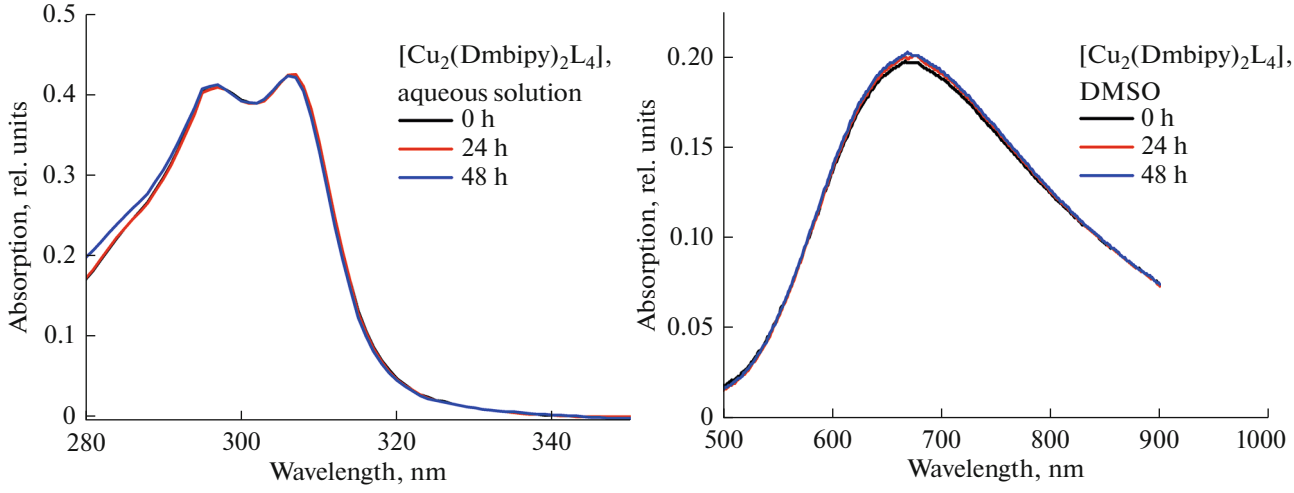

Fig. 10. Absorption spectra of complex **II** in the UV (aqueous solution) and visible (DMSO solution) spectral ranges.

Table 4. Values of IC_{50} for copper(II) acetate, HL, cisplatin, and complexes **I**–**V***

Compound	IC_{50}, μM			Selectivity index	
	cells Hep2	cells HepG2	cells MRC-5	cells Hep2	cells HepG2
$[Cu_2(Bipy)_2L_4]\cdot C_2H_5OH$ (**I**)	>50	35.0 ± 0.7	36.2 ± 2.2	>1	1.0
$[Cu_2(Dmbipy)_2L_4]$ (**II**)	12.4 ± 0.4	6.6 ± 0.2	12.0 ± 0.6	1.0	1.8
$[Cu_2(Phen)_2L_4]\cdot H_2O$ (**III**)	4.8 ± 0.4	3.6 ± 0.3	2.0 ± 0.8	0.4	0.6
$[Cu_2(Dmphen)_2L_4]$ (**IV**)	1.5 ± 0.1	1.8 ± 0.3	0.50 ± 0.06	0.3	0.3
$[Cu_2(Phendone')_2L_4]\cdot 2C_2H_5OH\cdot 2H_2O$ (**V**)	1.0 ± 0.1	0.92 ± 0.04	3.4 ± 0.3	3.4	3.7
Cisplatin	9.2 ± 0.5	33.0 ± 5.4	>50	>1	>1
HL	>50	>50	>100		
$Cu(OAc)_2$	>50	>50			

* The incubation time was 48 h.

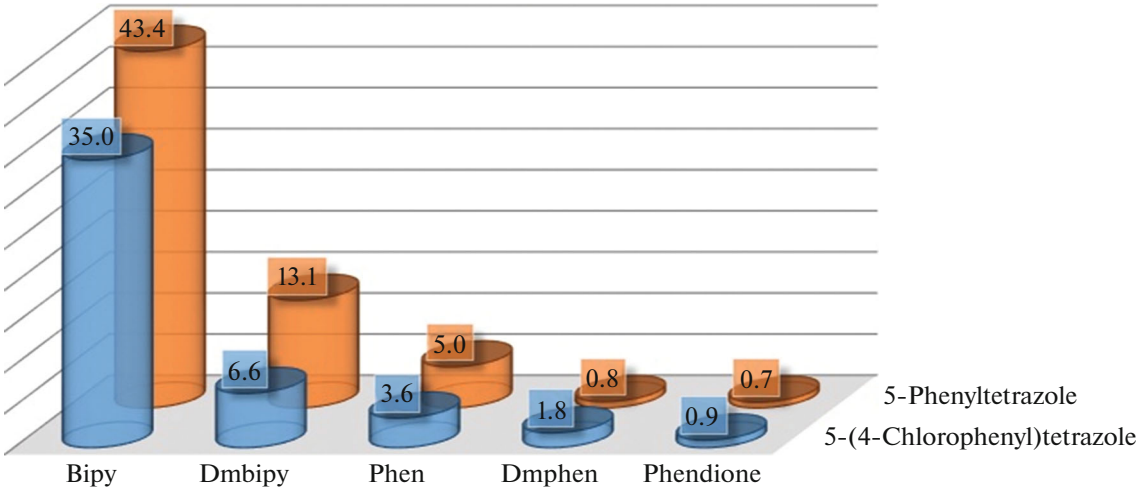

Fig. 11. Diagram with the parameters IC_{50} for the copper(II) complexes with different 2,2'-bipyridine/1,10-phenanthroline derivatives and 5-phenyltetrazole/5-(4-chlorophenyl)tetrazole.

no. 121031700321-3). The cytotoxic properties of the compounds were studied using the equipment of the Proteomic Analysis Center for Collective Use supported by the Ministry of Science and Higher Education of the Russian Federation (agreement no. 075-15-2021-691).

CONFLICT OF INTEREST

The authors declare that they have no conflicts of interest.

SUPPLEMENTARY INFORMATION

Additional information on this paper is available at https://doi.org/10.1134/S1070328423600110.

REFERENCES

1. Rosenberg, B., VanCamp, L., Trosko, J.E., et al., *Nature*, 1969, vol. 222, no. 5191, p. 385.
2. Ferraro, M.G., Piccolo, M., Misso, G., et al., *Pharmaceutics*, 2022, vol. 14, no. 5, p. 954.
3. González-Ballesteros, M.M., Mejía, C., and Ruiz-Azuara, L., *FEBS Open Bio*, 2022, vol. 12, no. 5, p. 880.
4. McGivern, T.J.P., Afsharpour, S., and Marmion, C.J., *Inorg. Chim. Acta*, 2018, vol. 472, p. 12.
5. Erxleben, A., *Coord. Chem. Rev.*, 2018, vol. 360, p. 92.
6. Molinaro, C., Martoriati, A., Pelinski, L., et al., *Cancers*, 2020, vol. 12, no. 10, p. 2863.
7. Kalinowski, D.S., Stefani, C., Toyokuni, S., et al., *Biochim. Biophys. Acta, Mol. Cell Res.*, 2016, vol. 1863, no. 4, p. 727.

8. Jiang, Y., Huo, Z., Qi, X., et al., *Nanomedicine*, 2022, vol. 17, no. 5, p. 303.
9. Pinheiro, A.C., Busatto, F.F., Schaefer, B.T., et al., *J. Inorg. Biochem.*, 2022, vol. 237, p. 112013.
10. Dinev, D., Popova, K.B., Zhivkova, T., et al., *Appl. Organomet. Chem.*, 2022, vol. 36, no. 10, p. e6862.
11. Cao, H.Z., Yang, W.T., and Zheng, P.S., *BMC Cancer*, 2022, vol. 22, no. 1, p. 1.
12. Babahan-Bircan, I., Emirdağ, S., Özmen, A., et al., *Appl. Organomet. Chem.*, 2022, vol. 36, no. 9, p. e6784.
13. Afroz, L., Khan, M.H.M., Vagdevi, H.M., et al., *Emergent Mater.*, 2021, vol. 5, no. 4, p. 1133.
14. Khursheed, S., Siddique, H.R., Tabassum, S., et al., *Dalton Trans.*, 2022, vol. 51, no. 31, p. 11713.
15. Santini, C., Pellei, M., Gandin, V., et al., *Chem. Rev.*, 2013, vol. 114, no. 1, p. 815.
16. Krasnovskaya, O., Naumov, A., Guk, D., et al., *Int. J. Mol. Sci.*, 2020, vol. 21, p. 3965.
17. Vitomirov, T., Dimiza, F., Matić, I.Z., et al., *J. Inorg. Biochem.*, 2022, vol. 235, p. 111942.
18. Figueroa-Depaz, Y., Pérez-Villanueva, J., Soria-Arteche, O., et al., *Molecules*, 2022, vol. 27, no. 11, p. 3504.
19. Karpagam, S., Mamindla, A., Kumar Sali, V., et al., *Inorg. Chim. Acta*, 2022, vol. 531, p. 120729.
20. Zehra, S., Cirilli, I., Silvestri, S., et al., *Metallomics*, 2021, vol. 13, no. 11, p. mfab064.
21. Zehra, S., Gómez-Ruiz, S., Siddique, H.R., et al., *Dalton Trans.*, 2020, vol. 49, no. 46, p. 16830.
22. Paixão, D.A., de Oliveira, B.C.A., Almeida, J.C., et al., *Inorg. Chim. Acta*, 2020, vol. 499, p. 119164.
23. Karpagam, S., Kartikeyan, R., Paravai, N.P., et al., *J. Coord. Chem.*, 2019, vol. 72, no. 18, p. 3102.
24. Alvarez, N., Mendes, L.F.S., Kramer, M.G., et al., *Inorg. Chim Acta*, 2018, vol. 483, p. 61.
25. Figueroa-DePaz, Y., Resendiz-Acevedo, K., Dávila-Manzanilla, S.G., et al., *J. Inorg. Biochem.*, 2022, vol. 231, p. 111772.
26. Kumari, J., Mobin, S.M., Mukhopadhyay, S., et al., *Inorg. Chem. Commun.*, 2019, vol. 105, p. 217.
27. Stoll, S. and Schweiger, A., *J. Magn. Reson.*, 2006, vol. 178, no. 1, p. 42.
28. *Bruker Apex3 Software Suite: Apex3, SADABS-2016/2 and SAINT. Version 2018.7-2*, Madison: Bruker AXS Inc., 2017.
29. CrysAlisPro 1.171.38.46. The Woodlands (TX), Rigaku Oxford Diffraction, 2015.
30. Sheldrick, G.M., *Acta Crystallogr., Sect. A: Found. Adv.*, 2015, vol. 71, no. 1, p. 3.
31. Sheldrick, G.M., *Acta Crystallogr. Sect. C: Struct. Chem.*, 2015, vol. 71, no. 1, p. 3.
32. Dolomanov, O.V., Bourhis, L.J., Gildea, R.J., et al., *J. Appl. Crystallogr.*, 2009, vol. 42, no. 2, p. 339.
33. Eremina, J.A., Lider, E.V., Samsonenko, D.G., et al., *Inorg. Chim. Acta*, 2019, vol. 487, p. 138.
34. Smirnova, K.S., Golubeva, Y.A., and Lider, E.V., *Cryst. Rep.*, 2022, vol. 67, no. 4, p. 575.
35. Eremina, J.A., Ermakova, E.A., Smirnova, K.S., et al., *Polyhedron*, 2021, vol. 206, p. 115352.

Translated by E. Yablonskaya